Available online at www.sciencedirect.com
ScienceDirect
Acta Materialia 56 (2008) 3699–3707
Acta MATERIALIA
www.elsevier.com/locate/actamat

Internal stress relaxation and load redistribution during the twinning–detwinning-dominated cyclic deformation of a wrought magnesium alloy, ZK60A

L. Wu [a,*], S.R. Agnew [b], D.W. Brown [c], G.M. Stoica [a], B. Clausen [c], A. Jain [b], D.E. Fielden [a], P.K. Liaw [a]

[a] Department of Materials Science and Engineering, University of Tennessee, Knoxville, TN 37996, USA
[b] Department of Materials Science and Engineering, University of Virginia, Charlottesville, VA 22904, USA
[c] Los Alamos National Laboratory, Los Alamos, NM 87545, USA

Received 14 February 2008; received in revised form 2 April 2008; accepted 3 April 2008
Available online 30 April 2008

Abstract

A study of the internal strain (stress) evolution during cyclic deformation dominated by $\{10\bar{1}2\}\langle 10\bar{1}1\rangle$ twinning and detwinning mechanisms within a magnesium alloy, ZK60A, was conducted using in situ neutron diffraction. It is shown that once the matrix grains twin, the (00.2) matrix and twin grains are relaxed relative to the neighbors. This load redistribution between the soft- and hard-grain orientations is a result of plastic anisotropy. The twins which formed during the initial compression sustain a tensile stress along the *c*-axis, when the applied compressive stress is less than ~80 MPa upon unloading. This local (intergranular) tensile stress is hypothesized to be effective for driving the detwinning event under a macroscopic compressive field along the *c*-axis. The activation stresses, 15 and 6 MPa, respectively, for the $\{10\bar{1}2\}\langle 10\bar{1}1\rangle$ extension twinning and detwinning, are approximated, based on the relaxation of the internal stresses in the matrix and twin grains.
Published by Elsevier Ltd on behalf of Acta Materialia Inc.

Keywords: Magnesium; Neutron diffraction; Deformation twinning; Internal strain

1. Introduction

Mg-based alloys have attracted extensive research efforts as potential lightweight structural materials with applications in the automotives, aircraft and electronics industries [1–8]. The important role of mechanical twinning in the plastic deformation of wrought magnesium alloys has been well recognized [6,9–11]. The strong anisotropy of hexagonal close-packed magnesium single crystals is due to the fact that the dominant slip mode, basal $\langle a\rangle$ slip, possesses only two independent slip systems, far from satisfying the five independent slip systems required by the von Mises criterion for an arbitrary homogeneous straining. In particular, the basal $\langle a\rangle$ slip cannot accommodate straining along the *c*-axis. Aside from the dislocation slips with $\langle c+a\rangle$ Burgers vectors, which are considered to be a very hard deformation mechanism [5], twinning is the only active deformation mode that can provide straining along the *c*-axis at room temperature. However, the $\{10\bar{1}2\}\langle 10\bar{1}1\rangle$ extension twinning can be easily activated by tensile stress along the *c*-axis. In common wrought magnesium alloys, most grains are oriented such that their *c*-axes are nearly perpendicular to the prior working direction; this favors significant $\{10\bar{1}2\}\langle 10\bar{1}1\rangle$ twinning under some loading conditions but not in others. This is the reason for the well-known tension–compression strength asymmetry of wrought magnesium alloys, where the strength in one direction is controlled by the stress required to activate

* Corresponding author.
E-mail address: lwu7@utk.edu (L. Wu).

1359-6454/$34.00 Published by Elsevier Ltd on behalf of Acta Materialia Inc.
doi:10.1016/j.actamat.2008.04.006

twinning, while the strength in the other is controlled by the harder non-basal slip mechanisms [12,13]. The unique orientation relationship between the parent grains and the twin grains (~90° reorientation) facilitates detwinning during the subsequent loading reversal [14–17]. Therefore, the plastic deformation during the cyclic loading of the common magnesium alloys at room temperature is dominated by twinning and detwinning mechanisms [14,16,18,19].

The mechanical response of polycrystalline metals is an average of the response of individual crystals (grains). In general, crystals exhibit both elastic and plastic anisotropy, which leads to load transfer between different grain orientations during loading. Because of the near elastic isotropy in magnesium alloys, the intergranular strains (the strain mismatch within different grain orientations) primarily arise from plastic anisotropy, which is controlled by the active slip and twinning systems. Therefore, a study of the internal strain evolution during the cyclic plastic deformation will give us more insight into the twinning and detwinning behavior in this material. The objective of the present paper is to provide experimental data necessary to develop a quantitative description of the load transfer mechanisms within magnesium alloys by reporting the development of internal strains during cyclic loading.

2. Experimental details

The magnesium alloy, ZK60A, sample used in this study was cut from a commercially extruded plate with T5 temper (partially solution-treated at 535 °C for 2 h, quenched in hot water, then aged at 185 °C for 24 h), which has a nominal composition of 6.0% Zn, 0.5% Zr (wt%), and Mg as balance. The crystallographic texture of the as-extruded plate has been reported elsewhere [14]. The initial texture exhibits two major texture components, one with the basal planes parallel to the plate and the other with the basal poles parallel to the transverse direction. Consequently, under the current loading condition, most grains in the sample are extensively twinned under the compressive loading along the extrusion direction and detwinned during the subsequent unloading and tensile reloading. In the current experimental setup, all the twin grains and the parent grains with their initial *c*-axes perpendicular to the plate normal are readily captured by in situ neutron diffraction, while those parent grains with their *c*-axes parallel to the plate transverse direction are not recorded.

In situ neutron-diffraction measurements were conducted on the spectrometer for materials research at temperature and stress (SMARTS) (Fig. 1) at the Los Alamos Neutron Science Center (LANSCE). The experimental details were described in Ref. [14] and only briefly presented here. The threaded-end sample with the loading axis parallel to the extrusion direction, having a 19.05 mm gage section with a 6.35 mm diameter, was mounted in the horizontal load frame. The prior plate normal was carefully aligned in the horizontal direction so that

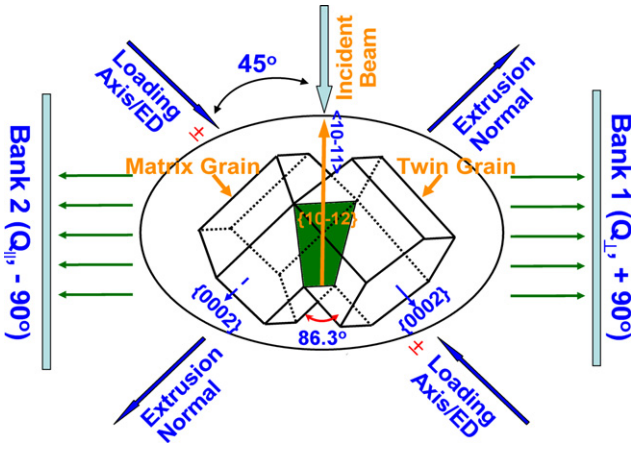

Fig. 1. A schematic of the SMARTS configuration at LANSCE. The loading axis is parallel to the extrusion direction (ED) of the extruded plate. The central part shows that the $\{10\bar{1}2\}\langle 10\bar{1}1\rangle$ extension twin system in magnesium results in an 86.3° reorientation of the twin grain relative to the parent grain.

a large volume fraction of grains have their basal poles in the diffraction plane (horizontal) but transverse to the loading direction. The loading axis was oriented at 45° relative to the incident beam, and the two detector banks situated at ±90° simultaneously record two complete diffraction patterns with diffraction vectors parallel ($\mathbf{Q}_{\parallel}$) and perpendicular ($\mathbf{Q}_{\perp}$) to the applied load (Fig. 1). The cyclic-loading experiment was performed using the customized Instron load frame under fully reversed cyclic-loading conditions, at the constant total strain amplitude of 1.2% with a triangular waveform at room temperature. The macroscopic strain was measured using an extensometer attached to the sample, and the imposed cyclic frequency was 0.5 Hz. The initial loading was compressive, which results in significant extension twinning during the first quarter cycle.

SMARTS uses polychromatic neutron beam and the time-of-flight (TOF) technique to record all possible lattice planes (effective *d*-space range from 0.03 to 0.4 nm), with their reflecting plane normals (scattering vectors) parallel or perpendicular to the loading axis. The configuration of SMARTS allows lattice strain evolutions in the parallel (longitudinal) and perpendicular (transverse) directions to the loading axis to be monitored simultaneously. In particular, the unique reorientation (~90°) associated with the extension twinning in magnesium alloys coupled with this configuration enables the separation of the daughter (twin) grain orientations from the parent (matrix) grain orientations [7,14,16,20]. For instance, the peaks diffracted from (00.2) planes in the longitudinal detector bank and (10.0) planes in the transverse detector bank are the direct detection of the daughter grains, while the parent grains can be characterized by the (10.0) peak in the longitudinal detector bank and the (00.2) peak in the transverse detector bank. Therefore, the development of the microstructure and stress state within the parent and daughter grains can be monitored simultaneously. Meanwhile, the

variation of peak intensity can signify a mechanical twinning and detwinning [14,16,19,21].

The internal strains can be calculated based on the peak shift of (hk.l) planes between the loaded and load-free patterns. Each reflection originates from a different family of grains, oriented such that the given (hk.l) plane diffracts to the detector banks. The average lattice strain for such grains is given by:

$$\varepsilon_{hk.l} = \frac{d_{hk.l} - d^0_{hk.l}}{d^0_{hk.l}} \quad (1)$$

where $d_{hk.l}$ and $d^0_{hk.l}$ are the plane d-spacings in the loaded and load-free conditions, respectively. However, due to the strong initial texture, some diffraction peaks [e.g. the (00.2) peak in the parallel direction and the (10.0) peak in the perpendicular direction] may initially be absent in one of the two banks (Fig. 1). In this case, we use the technique developed and successfully used for interpreting such data by Brown et al. [21] to obtain the d-spacing data for the load-free condition. For a load-free material that is elastically isotropic, the ratios between the given (hk.l) peak positions in banks 1 and 2 should be the same. These ratios are employed to obtain the lattice parameters for peaks initially absent in one of the banks. Nevertheless, certain peaks may be too weak in certain detector banks to give reliable internal-strain measurements, such as the (10.0) peak in the transverse direction with a large error bar (Fig. 5a and c).

3. Results and discussions

3.1. In situ neutron diffraction patterns

Fig. 2 represents the diffraction patterns from the parallel and perpendicular banks at various points (indicated in Fig. 3) along the hysteresis loop during the first deformation cycle. From the bottom to the top, the diffraction patterns correspond to (a) 0% (initial state), (b) −0.8% strain, (c) −1.2% strain, (d) 0 MPa stress, (e) −0.4% strain, (f) 0% strain, (g) +1.2% strain and (h) 0 MPa stress. Due to the strong texture, the initial diffraction peak reflected from the (00.2) basal planes is absent in the parallel detector bank, while it is strong in the perpendicular bank. The diffraction peak of the (10.0) prismatic planes is very weak in the perpendicular detector bank, but quite strong in the parallel detector bank, in the initial load-free diffraction patterns (see patterns "a" at the bottom in Fig. 2). The pyramidal (10.1) peaks are present in both detector banks. The initial diffraction spectra are consistent with the pole figures reported previously (see Fig. 2 in Ref. [14]), which were measured by conventional X-ray diffraction.

As discussed earlier, the in situ neutron diffraction patterns reveal a number of different aspects related to the evolutions of the microstructure and stress state in the sample. In Section 3.2 below, the cyclic twinning–detwinning behavior is briefly reviewed with relation to the intensity

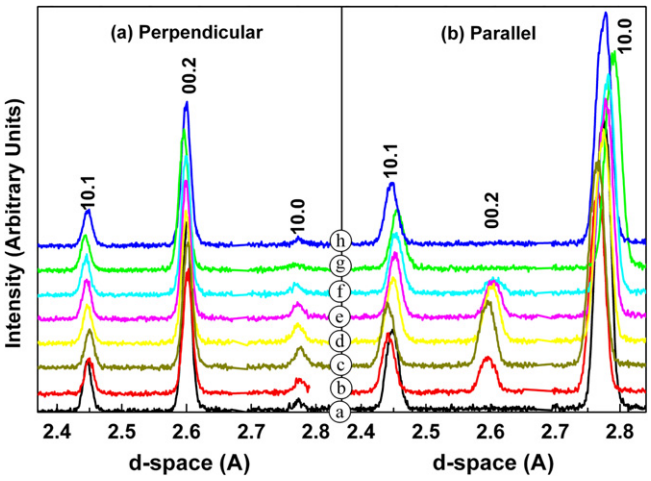

Fig. 2. Diffraction patterns during the first cycle deformation in parallel and perpendicular detector banks at various measuring points along the hysteresis loop (indicated in Fig. 3). The patterns have been offset vertically for clarity. The diffraction patterns correspond to: (a) 0% (initial state), (b) −0.8% strain, (c) −1.2% strain, (d) 0 MPa stress, (e) −0.4% strain, (f) 0% strain, (g) +1.2% strain and (h) 0 MPa stress.

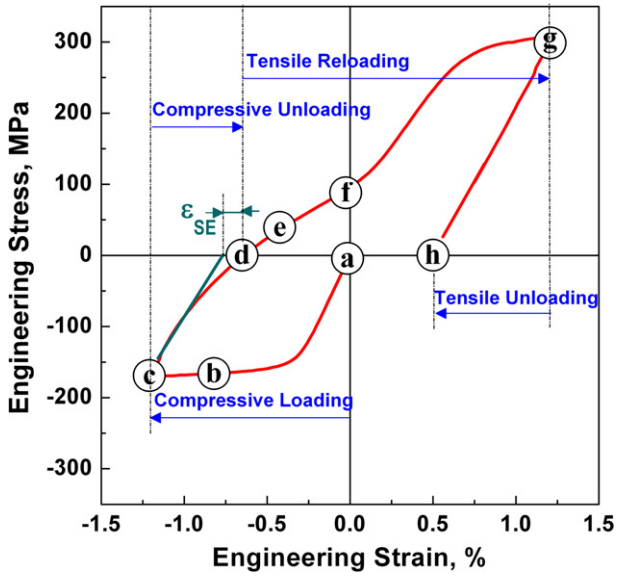

Fig. 3. An asymmetric hysteresis loop loaded along the prior extrusion direction for the first cycle, characteristic of twinning and detwinning in Mg alloy. The loop was divided into four loading stages – compressive loading, compressive unloading, tensile reloading and tensile unloading – as well as some that are letter labeled as the measuring points for later discussion. The figure also indicates the recoverable (or pseudo-elastic) strain, ε_{SE}.

changes of the diffraction peaks and the corresponding strangely shaped hysteresis loops. In Section 3.3, the internal strain (stress) evolutions derived from the peak shifts are examined in detail (the focus of this paper). Thereafter, the peak broadening is discussed in terms of intergranular and intragranular stresses (in Section 3.4). Finally, in Section 3.5, the activation stresses for twinning and

detwinning events are approximated, based on the relaxation of the internal stresses in the matrix and twin grains, respectively.

3.2. Macroscopic mechanical behavior

The macroscopic stress–strain response and cyclic twinning–detwinning behavior in this material when loaded along the prior extrusion direction have been published elsewhere [14]. The strangely shaped hysteresis loop for the first cycle shown in Fig. 3 is asymmetric with a sigmoidal shape, characteristic of twinning–detwinning behavior. This phenomenon is attributed to the formation of the $\{10\bar{1}2\}\langle 10\bar{1}1\rangle$ extension twins during the compressive loading and detwinning during the subsequent reversed loading, as evidenced by the intensity transfer of the basal (00.2) poles between the parallel and perpendicular detector banks. Twinning and detwinning alternate with the cyclic loading, and most twins formed during the compression are removed via detwinning when the load is reversed.

The fact that the detwinning is initiated prior to the compressive stress being completely unloaded (i.e. no tensile reloading is required) results in a Bauschinger-type non-linear unloading curve (Fig. 3). In this way, the extension twinning in magnesium is demonstrated to be a pseudo-elastic phenomenon [22,23], not unlike the stress-induced martensite formation observed in some shape memory alloys [24–26]. However, the recoverable (or pseudo-elastic) strain, ~0.13%, is quite small in the current case (indicated in Fig. 3). In contrast, the linear unloading curve from tension is due to the elastic deformation. This asymmetry between the compressive and tensile unloading in the hysteresis loop does not appear to be related to the fact that the total macroscopic strain imposed during tensile loading is more than the one imposed during the initial compression.

3.3. In situ measurement of internal-strain evolutions

It is worth emphasizing that each line in the plot of applied stress vs. lattice strain represents the response of a family of grains oriented such that the plane normal to the given (hk.l) lattice plane is parallel to the scattering vector. Because the diffraction technique detects only changes in the elastic "lattice" strain, the measured internal lattice strain is necessarily proportional to the stress on that grain, and the deviation from the linearity between applied stress and lattice strain indicates a stress redistribution among different grain orientations. When grains in a soft orientation micro-yield and, thus, share a smaller portion of the applied stress, a concomitant increase in the slope of the applied stress vs. internal strain curve is observed. A vertical line in these plots indicates that the grains of this orientation have ceased to accept elastic strains, and are behaving in a perfectly plastic fashion [20,27]. At the same time, grains in hard orientations must accept a larger portion of applied stress, and this is manifested as a decrease in slope.

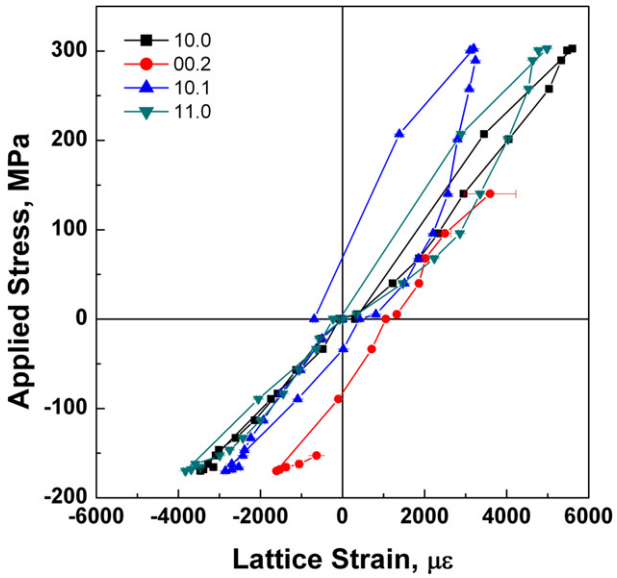

Fig. 4. Hysteresis loops of applied stress vs. lattice strain during the first cycle for the parallel direction. Due to the absence of a (00.2) peak at the initial and later stages during the first cycle, no internal strain data are available to form a complete loop for the basal (00.2) reflection. The different Bauschinger-type effects may be explained in terms of grain orientation and Schmid factor for basal slip.

Fig. 4 shows the hysteresis loops (applied stress vs. internal strain) for the four reflecting planes in the longitudinal direction during the first cycle of deformation. Different loop areas are observed for the various grain orientations, indicating different Bauschinger-type effects. The (10.0) grain orientation in the parallel direction has a much smaller Bauschinger effect than the (10.1) grain orientation. This difference may be explained in terms of the grain orientation and Schmid factor for the basal slip, e.g. a soft-grain orientation has a larger Bauschinger effect, while the effect is smaller for hard orientations. The following detailed discussion is based on Fig. 5, which shows internal strain evolutions during the first deformation cycle, respectively, for (a) initial compressive loading, (b) compressive unloading, (c) tensile reloading and (d) tensile unloading (see also Fig. 3).

The sample initially undergoes compressive elastic deformation and the internal strains (with a compressive sign) increase linearly with the macroscopic applied stress at nearly the same slope for all grain orientations (Fig. 5a), owing to the near-elastic isotropy of Mg. The slopes in the transverse direction are much steeper than those in the longitudinal direction as a result of the Poisson effect and the lack of an external boundary constraint [28]. The basal plane in the (10.1) grain orientations is inclined at an angle of 28° to the loading axis yielding a Schmid factor of ~0.305 for basal slip. Thus, this subset of grains is favorably oriented for basal $\langle a\rangle$ slip (e.g. in a soft orientation) relative to their neighbors. They yield first, and smaller elastic strains are observed in the yielded grains, so that the corresponding curve diverges from the linear response

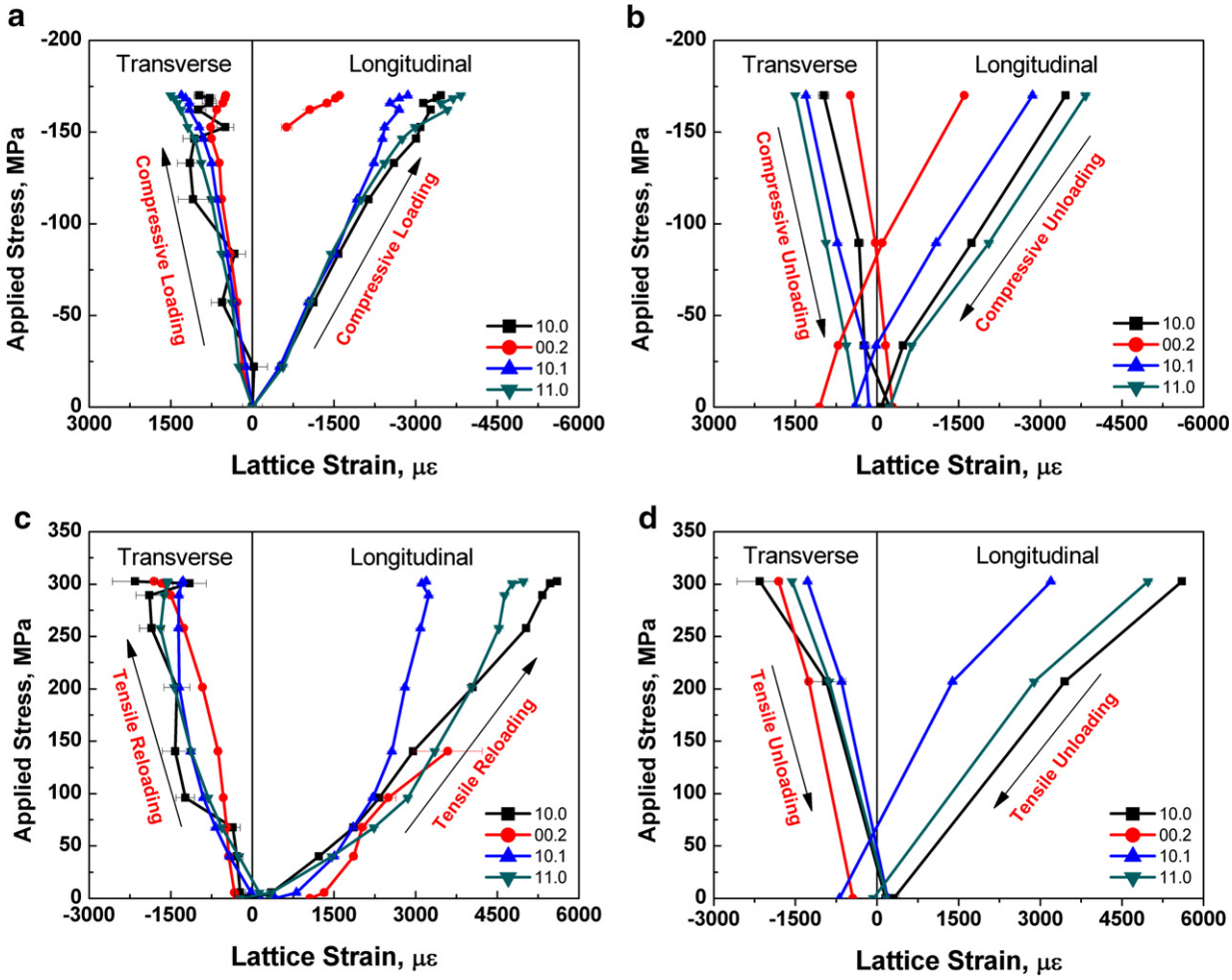

Fig. 5. Internal strain evolutions for, respectively, (a) initial compressive loading, (b) compressive unloading, (c) tensile reloading and (d) tensile unloading during the first cycle, indicated in Fig. 3. The internal strain (stress) evolution in the different grain orientations can be understood in terms of load transfer among those grain orientations.

with an increasing slope. A similar transition occurs for the (10.1) grain orientation in the transverse direction. It can be deduced that the other subset of grains, in hard orientations, share a larger portion of load and their associated slopes decrease. This behavior can be understood largely in terms of the elastic load transfer between soft- and hard-grain orientations behaving like a composite material [29]. However, the volume fraction of (10.1) grains is small in this strongly textured material, and thus their effect on the overall behavior is small. This trend agrees well with the reports by the groups of Agnew, Brown and Clausen [20,21,27,30] for the extruded magnesium alloy, AZ31B, under monotonic compressive loading. When the sample starts to macroscopically plastically deform by twinning at the stress of ~ -150 MPa, a (00.2) peak in the parallel bank appears (Fig. 5a), and thereafter the lattice strain in the twins can be calculated accordingly.

Once the twinning is activated, the (00.2) parent grains (see the transverse direction in Fig. 5a) are relaxed relative to the stress field in the surrounding grains. Therefore, the (10.0) and (11.0) parent grains (Fig. 5a, in the longitudinal direction) share more stress, and their slopes of the internal strain curves decrease. The newly formed daughter grains (see the (00.2) reflection in the longitudinal direction in Fig. 5a) have a much smaller stress than the other grains. However, the twins are in a plastically hard orientation with respect to basal slip. Therefore, the stress within the twins accumulates very quickly. It was suggested previously [14] that the twins and parents must contain significant internal stresses that drive the detwinning event to occur immediately upon unloading (i.e. it does not require reverse loading). The measured internal strains (stresses) in Fig. 5a have confirmed this hypothesis.

During the unloading from the maximum compressive stress, the lattice strains in all observed grain orientations (hk.l) change at the same pace (another expression of elastic isotropy and evidence that little plastic unloading occurs). However, the internal stress state in the daughter grains along the parallel direction (see the (00.2) reflection in the longitudinal direction in Fig. 5b) changes its sign at ~ -80 MPa. Beyond this point, the (00.2) daughter grains are placed in a tensile stress field along their *c*-axis, which

is effective in driving the detwinning event. At zero applied stress, the (00.2) daughter grains are in a much greater tensile stress field along their *c*-axes compared to the other grain orientations (Fig. 5b, in the longitudinal direction). In fact, it is a sufficient level of stress to initiate detwinning. Detwinning is a mechanism of plastic deformation, so this is an example of a classical Bauschinger effect in that plastic deformation occurs at a lower absolute stress during reloading than it did during the initial monotonic loading. In this case, intergranular stresses that arise due to plastic anisotropy appear to assist the Bauschinger effect.

When the sample is reloading in tension, the detwinning dominates the plastic deformation until the twins appear to be completely removed at an applied stress of ~100 MPa (Fig. 3). Once the sample is completely detwinned, the resulting orientation is again hard with respect to tensile deformation by the basal slip. This demands the activation of the harder non-basal dislocation slip [5] or $\{10\bar{1}1\}\langle 10\bar{1}\bar{2}\rangle$ compressive twinning mechanisms [8,19,27]. However, the grains in a soft orientation, such as (10.1) grains in the parallel direction, again micro-yield, and their corresponding curve departs from linearity (Fig. 5c). These grains stop to accept more internal stresses, while other subsets of grains continue to take more internal stresses.

Although we already have discussed the internal strain evolution in detail above, based on Fig. 5, the correlation between the internal strains and the twinning–detwinning behaviors can be more clearly observed in Fig. 6, which shows the internal strain evolution in both the longitudinal and transverse directions as a function of the macroscopic strain for the first few cycles. Also included is a curve of the (0002) pole intensity evolution, which provides a measure of the volume fraction of twinning and detwinning [14]. Once twinning is activated and twin grains appear, the internal stresses both in the longitudinal and transverse directions are relaxed and, subsequently, increase more slowly with the macroscopic strain. The internal strain accumulation in the (00.2) parent grains (see the transverse direction) especially decrease due to the significant stress relaxation. When the twinned grains are exhausted at the strain of ~0%, plastic deformation continues through the activation of the harder prismatic or pyramidal dislocation slips and the internal stresses in both directions accumulate more quickly. However, as discussed above, because the (10.1) grains are oriented favorably for the basal slip, the internal strain in those grains rise more slowly than in the other grain orientations. The twinning and detwinning behavior clearly play a significant role in the cyclic deformation of this material, and these mechanisms are in turn significantly affected by the generation and relaxation of internal strains (stresses).

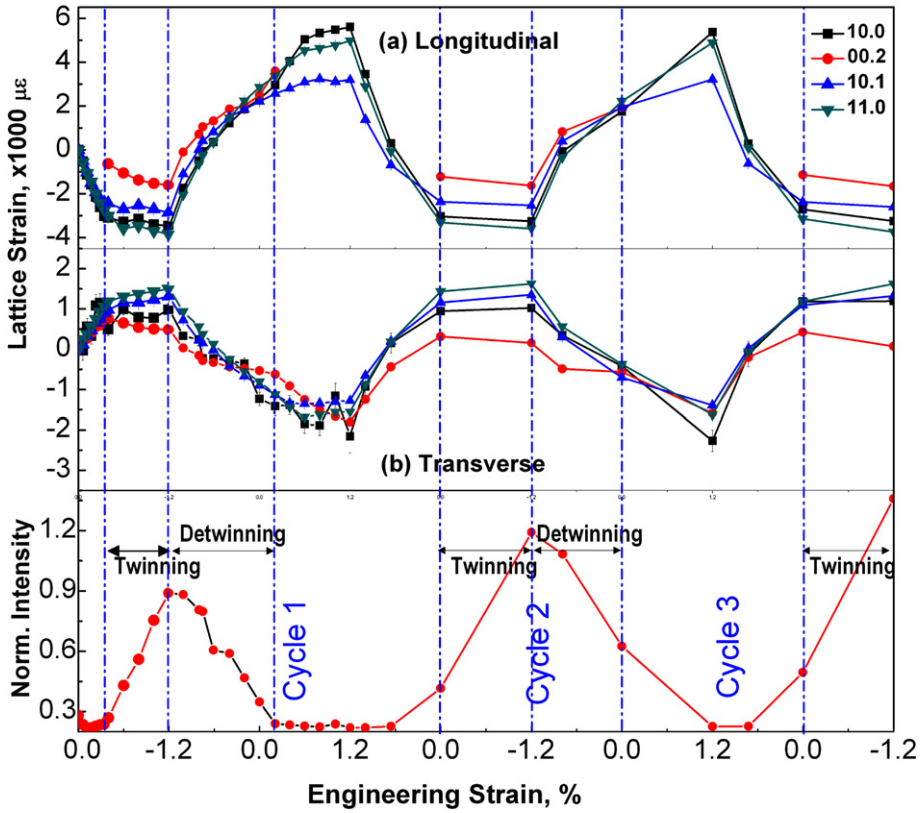

Fig. 6. Lattice strain evolution as a function of engineering strain for the first few cycles. Also included is a curve of the (0002) pole intensity evolution in the parallel bank, which is a direct measure of twin grains, indicating the cyclic twinning and detwinning behavior. The correlation between the internal strains and the twinning–detwinning behavior can be clearly observed.

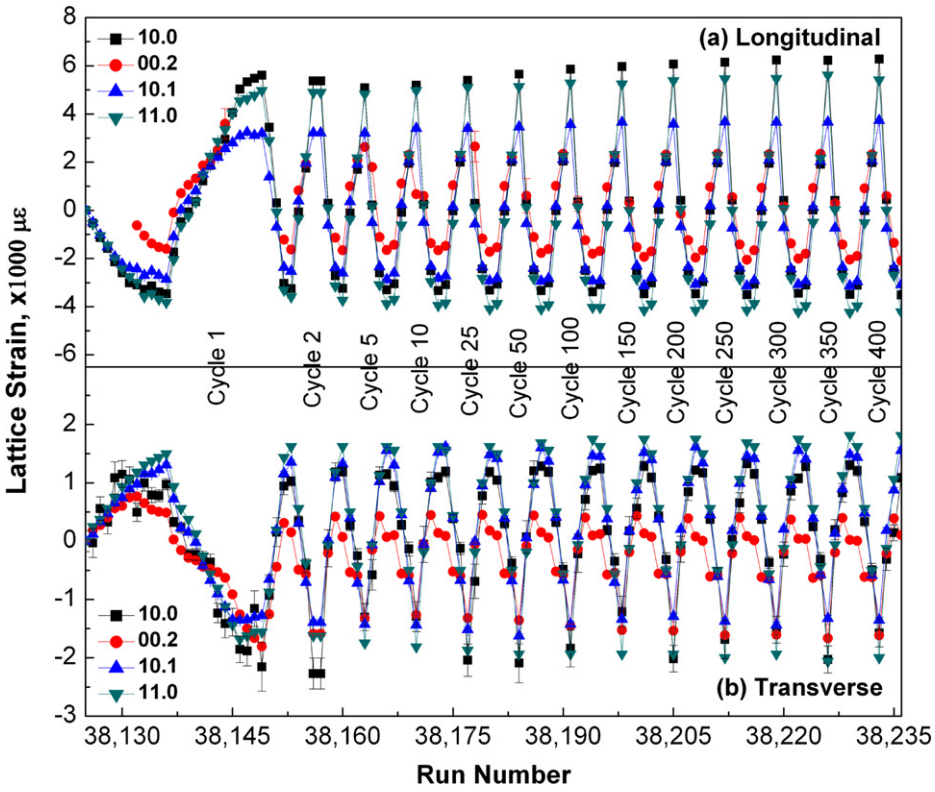

Fig. 7. Lattice strains as a function of run number, indicating cyclic evolution of lattice strains: (a) in the longitudinal direction; (b) in the transverse direction. The internal strain development in the following cycles closely follows the evolution during the first cycle deformation.

The cyclic evolution of the internal lattice strains is shown in Fig. 7, which is an extension of Fig. 6 to include more cycles. The lattice strains for the four grain orientations are plotted as a function of the "run number", which is used for experimental bookkeeping to identify the diffraction data. We can conclude that the internal strain development in the following cycles closely follows the evolution during the first cycle deformation. Nevertheless, the amplitude of the internal strains (stresses) gradually escalate with increasing cycle number (Fig. 7). The rise in internal strain with cycles is a form of cyclic hardening due to exhaustion of the twinning–detwinning mechanism.

In summary, the internal strain (stress) evolutions in the different grain orientations observed via in situ neutron diffraction measurements (see Figs. 4–7) can be understood in terms of load transfer among those grain orientations, where the twinning and detwinning behaviors play an important role.

3.4. Peak broadening

In addition to changes in peak intensity and peak position, the neutron diffraction data also manifest that there are changes in peak width. Fig. 8 shows the broadening of the (00.2), (10.1) and (11.0) reflections, both parallel and perpendicular to the loading axis, as a function of run number. Both in the longitudinal and transverse directions, the (00.2) grain orientation has the largest overall peak broadening, while the (11.0) grain orientation has the smallest overall peak broadening. In the present study, the most significant contributing factors to the peak broadening are (i) grain-to-grain variations in the intergranular stresses (the focus of this paper) and (ii) intragranular stresses due to dislocations [21,31]. Because of the dominated twinning deformation, many dislocations are present in the (00.2) grain orientation due to accommodation requirements during twinning, and this leads to the largest peak broadening. This statement is further corroborated by the fact that the (00.2) peak broadening develops cyclically with the twinning and detwinning alternately active (Fig. 8). The (10.1) grains in both detector banks are in a soft orientation with respect to the activation of basal slip system. Hence, there are more basal dislocations in these grains than in other grains in a hard orientation, such as the (11.0) grain orientation, which has the smallest peak broadening. Finally, the overall peak broadening gradually increases with continued cycling, which indicates an accumulation of residual twins and/or dislocations. In fact, a small volume fraction of residual twins (twins which fail to detwin completely) was detected, which gradually increases with increasing cycles (see Fig. 6 in Ref. [14]). Furthermore, the mutual interactions between the twin boundaries and dislocation slips are related to the applied cyclic stress reported previously (please see Fig. 5 in Ref. [14]) and, correspondingly, the amplitude of the internal strains (stresses) (Fig. 7).

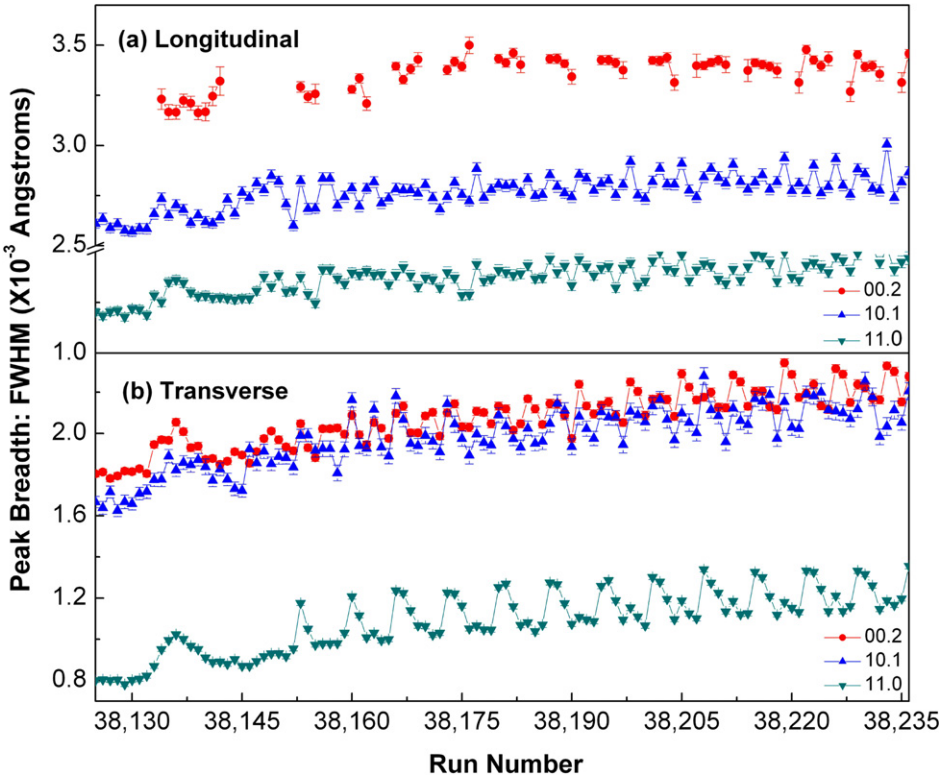

Fig. 8. Broadening of diffraction peaks as a function of run number along the longitudinal direction (a) and along the transverse direction (b). The peak broadening in the current study is mostly related to the volume of twins and dislocations in the material.

3.5. Approximation of the activation stresses

In general, it has been assumed that, like dislocation slip, deformation twinning is primarily controlled by the resolved shear stress on the twin plane and in the twinning direction [32], thus a Schmid law is assumed and given by:

$$\tau_{\mathrm{CRSS}} = \sigma_{\mathrm{c}} \cos\lambda \cos\chi \tag{2}$$

where λ and χ are the angles between the loading axis and the twin plane normal and twin direction, respectively, and σ_{c} and τ_{CRSS} are the critical applied stress and the critical resolved shear stress (CRSS). Gharghouri et al. [19] demonstrated the validity of this assumption for the $\{10\bar{1}2\}\langle 10\bar{1}1\rangle$ extension twinning in magnesium and reported a CRSS value of 65–75 MPa in the Mg–7.7 at.% Al alloy. The uniaxial form of the Schmid law listed above schematically represents the full tensorial relationship, where the tensorial stress applied at the grain level is resolved in a similar way using the Schmid tensor (the dyadic cross product of the twin plane normal and twin shear direction). For simplicity of presentation, we have assumed that the stress state at the grain level is uniaxial; however, it is recognized that the local stresses depart from those applied to the aggregate.

As stated above, the internal stress in the (00.2) parent grains in the transverse direction (Fig. 5a) linearly increases during the initial compression until the extension twinning is activated, at which point the internal stress in the (00.2) parent grains is relaxed (see Fig. 6, in the longitudinal direction). Thus a maximum internal stress observed within the (00.2) parent grains (see Fig. 5a, in the transverse direction) can be reasonably employed for the calculation of the activation stress for extension twinning. In the current measurement, the maximum internal strain of the parent (00.2) grains is 770 με, which suggests a stress of 37 MPa via the uniaxial Hooke's Law, given the (00.2) specific elastic modulus of 48 GPa [21] for magnesium. The activation stress is thus the resolved shear stress, 15 MPa, along the twinning direction $\langle 10\bar{1}1\rangle$ in the twinning plane $\{10\bar{1}2\}$ with a Schmid factor of ~0.40. This activation stress agrees well with the value of 15 MPa employed by Agnew et al. [8] for the viscoplastic self-consistent simulation of an AZ31B magnesium alloy, while in the elastoplastic self-consistent model, initial values of 30 and 54 MPa, respectively, are assumed by Agnew et al. [20] and by Clausen et al. [30] for the same alloy with different models to account for the effects of twinning.

The stress–strain response departs from the linear elasticity almost immediately, indicating the onset of detwinning even at a strain of −1.0% (see Fig. 7 in Ref. [14]). However, when the sample is further unloaded to a strain of −0.8%, the rate of detwinning increases. This point is further evidenced in Fig. 6, which shows that the internal strain curve for the (00.2) twin grain orientation between −1.0 and −0.8% strain (see the longitudinal direction) has a lower slope than that between −1.2 and −1.0%

strain. This indicates that the (00.2) twin grains relax more quickly due to a higher detwinning rate. Consequently, the internal stress in the twin grains at a strain of −0.9%, 15 MPa (e.g. an internal strain of 310 με), can be again resolved to a shear stress, 6 MPa, along the twinning direction $\langle 10\bar{1}1\rangle$ in the twinning plane $\{10\bar{1}2\}$, roughly as the activation stress for detwinning event, which is lower than that of twinning. This result agrees qualitatively with the observations in the alloy, AZ31B [15,16]. The difference between the activation stresses of twinning and detwinning events is 9 MPa, which places the present directly measured result in quantitative agreement with the number derived theoretically by Lou et al. [15].

4. Summary and conclusions

The cyclic deformation of wrought magnesium alloys is dominated by twinning and detwinning due to the unique reorientation of the extension twinning with respect to the initial basal texture. The configuration of SMARTS is advantageous for studying the internal strains (stresses) in the parent grains and twin grains separately in the magnesium alloys. The strong texture in the most common magnesium alloys places most grains in a hard orientation relative to stresses acting along the prior extrusion direction, though there is a small volume fraction of grains in a soft orientation in the present case. While extension twinning is active, the load-induced internal stresses in the (00.2) parent and twin grains are relaxed, and they are significantly smaller compared to the internal stresses in the other grain orientations. The difference in internal stress levels is attributed to the plastic anisotropy, and this ultimately dominates twinning and detwinning behavior. This kind of load transfer is a typical phenomenon in polycrystal metals [33] and composite materials [29]. The significant internal (intergranular) tensile residual stress generated in the material during twinning drives the detwinning event during the compressive unloading (i.e. no tensile reloading is required). In this way, extension twinning is a pseudo-elastic phenomenon, not unlike the stress-induced martensite formation observed in some shape memory alloys. However, the recoverable strain is quite small.

Finally, the activation stresses for the $\{10\bar{1}2\}\langle 10\bar{1}1\rangle$ extension twinning and detwinning were calculated based on the internal strains at which twinning or detwinning begins to be active for plastic deformation. The activation stresses for the extension twinning and detwinning event are determined to be 15 and 6 MPa, respectively.

Acknowledgements

The authors are grateful for the financial support from the National Science foundation – Combined Research and Curriculum Development (CRCD) Program under EEC-9527527, with Ms. M. Poats as the Program Director, and the National Science Foundation – International Materials Institute (IMI) Program under DMR-0231320, with Dr. C. Huber as the Program Director. S.R.A. is sponsored by a subcontract from the Los Alamos National Laboratory funded by the Office of Basic Energy Science (DOE) through Project FWP 06SCPE401. The Los Alamos Neutron Science Center (LANSCE) is a national user facility funded by the United States Department of Energy, the Office of Basic Energy Science – Materials Science, under Contract No. W-7405-ENG-36 with the University of California.

References

[1] Agnew SR, Mehrotra P, Lillo TM, Stoica GM, Liaw PK. Acta Mater 2005;53:3135–46.
[2] Agnew SR, Mehrotra P, Lillo TM, Stoica GM, Liaw PK. Mater Sci Eng A 2005;408:72–8.
[3] Liaw PK, Ho TL, Donald JK. Scripta Metall 1984;18:821–4.
[4] Wu L, Stoica GM, Liao H-H, Agnew SR, Payzant EA, Wang G, et al. Metall Mater Trans A 2007;38:2283–9.
[5] Agnew SR, Duygulu O. Int J Plasticity 2005;21:1161–93.
[6] Jain A, Agnew SR. Mater Sci Eng A 2007;462:29–36.
[7] Brown DW, Agnew SR, Abeln SP, Blumenthal WR, Bourke MAM, Mataya MC, et al. Icotom 14: Texture Mater 2005;495–497(Pts 1 and 2):1037–42.
[8] Agnew SR, Yoo MH, Tome CN. Acta Mater 2001;49:4277–89.
[9] Yoo MH. Metall Trans A 1981;12:409–18.
[10] Roberts CS. Magnesium and its alloys. New York: John Wiley & Sons Inc.; 1960.
[11] Yoo MH, Lee JK. Philos Mag A 1991;63:987–1000.
[12] Avedesian MM, Baker H. Magnesium and magnesium alloys (ASM specialty handbook). Materials Park, OH: ASM International; 1999.
[13] Barnett MR. Mater Sci Eng A 2007;464:1–7.
[14] Wu L, Jain A, Brown DW, Stoica GM, Agnew SR, Clausen B, et al. Acta Mater 2008;56:688–95.
[15] Lou XY, Li M, Boger RK, Agnew SR, Wagoner RH. Int J Plasticity 2007;23:44–86.
[16] Brown DW, Jain A, Agnew SR, Clausen B. Mater Sci Forum 2007;539–543:3407–13.
[17] Kleiner S, Uggowitzer PJ. Mater Sci Eng A 2004;379:258–63.
[18] Oliver EC, Daymond MR, Withers PJ. Mater Sci Forum 2005;490–491:257–62.
[19] Gharghouri MA, Weatherly GC, Embury JD, Root J. Philos Mag A 1999;79:1671–95.
[20] Agnew SR, Tome CN, Brown DW, Holden TM, Vogel SC. Scripta Mater 2003;48:1003–8.
[21] Brown DW, Agnew SR, Bourke MAM, Holden TM, Vogel SC, Tome CN. Mater Sci Eng A 2005;399:1–12.
[22] Caceres CH, Sumitomo T, Veidt M. Acta Mater 2003;51:6211–8.
[23] Wang XX, Zhang CY. J Mater Sci Lett 1998;17:1795–6.
[24] Daly S, Ravichandran G, Bhattacharya K. Acta Mater 2007;55:3593–600.
[25] Hamilton RF, Sehitoglu H, Efstathiou C, Maier HJ, Chumlyakov Y. Acta Mater 2006;54:587–99.
[26] Orgeas L, Favier D. Acta Mater 1998;46:5579–91.
[27] Agnew SR, Brown DW, Tome CN. Acta Mater 2006;54:4841–52.
[28] Lorentzen T, Daymond MR, Clausen B, Tome CN. Acta Mater 2002;50:1627–38.
[29] Allen AJ, Bourke MAM, Dawes S, Hutchings MT, Withers PJ. Acta Metall Mater 1992;40:2361–73.
[30] Clausen B, Tomé CN, Brown DW, Agnew SR. Acta Mater 2008. doi:10.1016/j.actamat.2008.01.057.
[31] Ungar T. Scripta Mater 2004;51:777–81.
[32] Reed-Hill RE, Abbaschian R. Physical metallurgy principles. 3rd ed. Boston, MA: PWS Publishing Company; 1994. p. 4143–4153.
[33] Daymond MR, Bourke MAM, VonDreele RB, Clausen B, Lorentzen T. J Appl Phys 1997;82:1554–62.